

Relative shift in position of temperature and density pedestals at the COMPASS tokamak

P. Bílková¹, P. Böhm¹, M. Komm¹, L. Frassinetti², E. Štefániková², M. Peterka^{1,3}, M. Šos^{1,4}, J. Seidl¹, O. Grover^{1,4}, J. Havlíček¹, K. Mitošinková^{1,3}, J. Varju¹, P. Vondráček^{1,3}, J. Urban¹, M. Imríšek¹, T. Markovič¹, V. Weinzettl¹, M. Hron¹, R. Pánek¹ and the EUROfusion MST1 team⁵

1 Institute of Plasma Physics of the CAS, Za Slovankou 3, 182 00 Prague 8, Czech Republic

2 KTH, Div Fus Plasma Phys, SE-10044 Stockholm, Sweden

3 Fac. Math & Phys., Charles University, V Holešovičkách 2, 180 00 Prague 8, Czech Republic

4 FNSPE, Czech Technical University in Prague, Břehová 7, Czech Republic

5 See author list in H. Meyer et al., Overview of progress in European Medium Sized Tokamaks towards an integrated plasma-edge/wall solution", accepted for publication in Nuclear Fusion

Introduction

Recent analysis performed on ASDEX Upgrade, NSTX and DIII-D suggest that the density profile position plays an important role in pedestal stability [1,2,3]. On JET and ASDEX Upgrade, it has been observed that the electron temperature and electron density profiles can have different relative pedestal positions (so-called relative shift). As shown in [4,5], the increase of the relative shift is correlated with the reduction in the normalized pressure gradient, leading to a weakening of the pedestal stability. Therefore, in this work, analysis of the effect of the relative shift has been carried on the COMPASS tokamak discharges.

The dataset used for analysis was obtained during two dedicated experimental campaigns in 2015 and 2016 [6]. Systematic measurements of pedestal structure were performed in Ohmic and NBI-assisted Type I ELM My H-modes [7]. For P_{NBI} exceeding 200 kW the electron pedestal temperature reached 300 eV, allowing to achieve pedestal collisionality $\nu_{ped}^* < 1$ at $q_{95} \sim 3$. Measurements during the last 30% of the ELM cycle were considered for analysis.

Diagnostics and analysis

Profiles of electron temperature and density measured by High Resolution Thomson Scattering (HRTS) system on COMPASS [8] are used to analyze the pedestal structure. This is a well-suited diagnostic for this purpose because it is capable to measure both electron density and temperature

simultaneously with sufficient spatial resolution, giving accurate information on relative shift between density and temperature pedestal positions. Profiles in pre-ELM phase were chosen for analysis as ELMs cause a periodic collapse of pedestal. Pre-ELM profiles were selected in the 70-99% of the ELM cycle. The measured profiles were fitted with the modified hyperbolic tangent (mtanh) function [9] using dedicated routines [10, 11]. The fits provide pedestal parameters such as height, width and position. Pedestal relative shift was calculated as a difference between the middle positions of electron density and electron temperature pedestals. A dataset with following range of dimensionless parameters was chosen: normalized collisionality ν^* lower than 2, q_{95} in the range (2.8, 3.2) and normalized thermal pressure β in the range (0.10, 0.35). The experimental normalized pressure gradient α_{exp} was calculated in a same way as in [4]:

$$\alpha = -\frac{2\partial_\psi V}{(2\pi)^2} \left(\frac{V}{2\pi^2 R_0} \right)^{1/2} \mu_0 p' \quad (1)$$

Results

Figure 1a shows dependence of pedestal widths of electron temperature T_e , electron density n_e and electron pressure p_e on pedestal density. Widths are shown in % of normalized poloidal flux ψ_N . Pedestal density width slightly increases with pedestal density. Values of density pedestal widths in absolute values (Fig. 1b) are similar to those measured at JET and DIII-D [12, 13] where the width values were in a range of 1-3 cm. Pedestal position shift versus power over separatrix P_{sep} is shown at Figure 2. There is a linear increasing trend between shift and P_{sep} as was also observed at JET [4]. Dependence of α_{exp} versus relative pedestal shift was investigated at JET [4] for a set of plasma with ν^* in the range 0.1-0.35. The low ν^* data well aligns with the JET. However, quantitatively the α_{exp} of COMPASS is lower than the one JET, in particular at low relative shift. This might be, at least in part, explained by the large collisionality of the COMPASS dataset compared to the JET one, see for example [14].

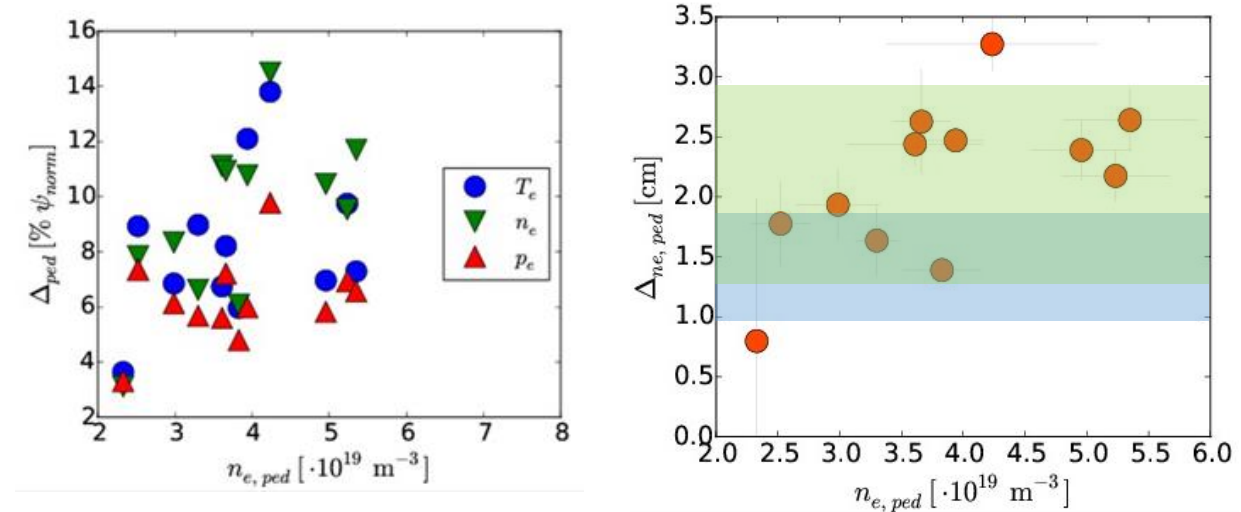


Fig. 1a Widths of kinetic profile pedestals in % ψ_{norm} versus pedestal electron density. Fig. 1b Width of electron density pedestal in absolute units versus pedestal electron density. Blue area indicates data from DIII-D, green area data from JET [12]

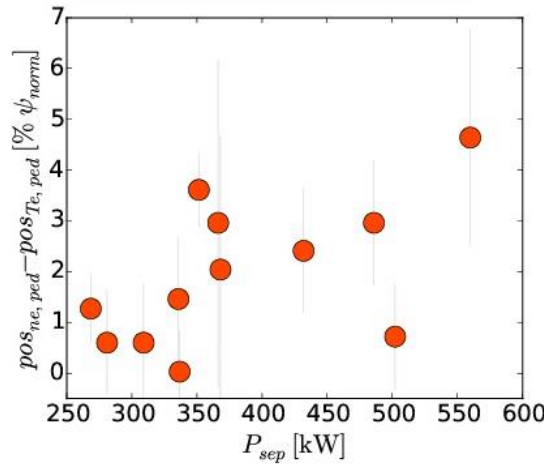


Fig. 2 Relative pedestal shift versus power over separatrix

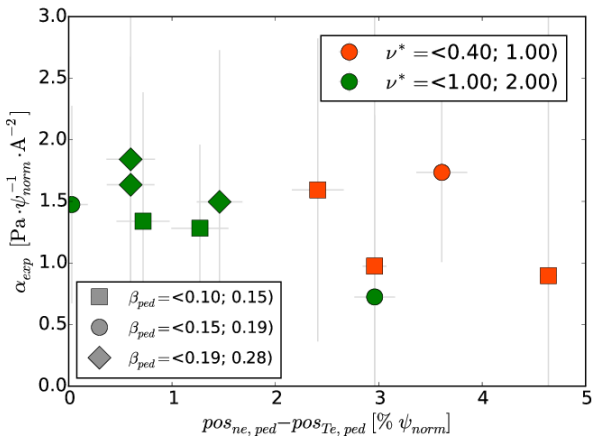


Fig. 3 Experimental normalized pressure gradient α_{exp} versus relative pedestal shift on COMPASS for different ranges of v^* and β_{pol}

Discussion / Conclusion

The absolute values of density pedestal widths are similar to those measured at JET and DIII-D. It suggests that width does not scale with plasma size. However, the values of relative shift of pedestal position in percent ψ are similar to JET which suggests that the relative shift does scale with plasma size, unlike the pedestal width. As COMPASS is smaller than JET, demands on measurement precision are higher. For low collisionality experiments, the α_{exp} data in dependence with relative pedestal shift well aligns with the JET.

Acknowledgements

This work was supported by grant GA14-35260S and co-funded by MEYS project number 8D15001. This work has also been carried out within the framework of the EUROfusion Consortium (MST1) and has received funding from the Euratom research and training programme 2014-2018 under grant agreement No 633053. This work has also been carried out within the framework of the EUROfusion Consortium (MST1). The views and opinions expressed herein do not necessarily reflect those of the European Commission.

References

- [1] T.H. Osborne et al., Nucl. Fusion **55**, 063018 (2015)
- [2] R. Maingi et al., Nucl. Fusion **52** 083001 (2012)
- [3] M. Dunne et al., Plasma Phys. Control. Fusion **59** (2017)
- [4] E. Stefanikova et al., 43rd EPS Conf. On Plasma Physics (Leuven, Belgium) O4.117
- [5] L. Frassinetti et al., Plasma Physics and Controlled Fusion **59**(1):014014 (2017)
- [6] R. Panek et al., Plasma Phys. Contr. F. **58** (2016) 014015
- [7] M. Komm et al., submitted to Nuclear Fusion (2016)
- [8] P. Bohm et al., Rev. Sci. Instrum. **85**, 11E431 (2014)
- [9] R.J. Groebner et al., Nucl. Fusion **41** 1789 (2001)
- [10] L. Frassinetti et al., Rev. Sci. Instrum. **83**, 013506 (2012)
- [11] E. Stefanikova et al., Rev. Sci. Instrum. **87**, 11E536 (2016)
- [12] M. Beurskens et al., Phys. Plasmas **18**, 056120 (2011)
- [13] P.A. Schneider et al., PPCF **54** (2012) 105009
- [14] L. Frassinetti et al., Nucl. Fusion **57** (2017) 016012
- [15] P. Wilson et al., Phys. Plasmas **9** 1277 (2002)